Physica Scripta

PAPER

The effect of giant Kerr nonlinearity on group velocity in a six-level inverted-Y atomic system

To cite this article: Le Van Doai 2020 *Phys. Scr.* **95** 035104

IOP Publishing Physica Scripta
Phys. Scr. 95 (2020) 035104 (7pp) https://doi.org/10.1088/1402-4896/ab5288

The effect of giant Kerr nonlinearity on group velocity in a six-level inverted-Y atomic system

Le Van Doai

Department of Physics, Vinh University, 182 Le Duan Street, Vinh City, Vietnam

E-mail: doailv@vinhuni.edu.vn

Received 4 September 2019, revised 10 October 2019
Accepted for publication 28 October 2019
Published 29 January 2020

Abstract

We propose an analytical model to study the effect of giant Kerr nonlinearity on group velocity of probe light in a six-level inverted-Y atomic system under electromagnetically induced transparency (EIT). In this scheme, a nonlinearity of the medium is enhanced greatly around in three spectral regions corresponding to transparent windows. As a consequence, such a giant Kerr nonlinearity of the medium changes significantly group index for probe light which can obstruct light slowdown. Moreover, this model shows also that the probe propagation can switch between subluminal and superluminal modes in three EIT windows by adjusting the parameters of the signal and coupling fields. Such analytical model is not only convenient for considering the influence of laser parameters on group velocity but is also easy used to fit the experimental results.

Keywords: electromagnetically induced transparency, group velocity, cross-Kerr effect

(Some figures may appear in colour only in the online journal)

1. Introduction

One of the exciting effects is generated by quantum coherence and interference in multi-level atomic systems as electromagnetically induced transparency (EIT) [1]. In addition to eliminated resonant absorption, the EIT effect can create giant Kerr-nonlinearity [2–6] and subluminal and superluminal light propagations [7–11]. Such a giant cross-Kerr nonlinearity associated with controllable group velocity have many applications in quantum phase gates [12–15], fast-phase switching [16], storage and retrieval of the light pulse [17], plasmonic wave propagation [18, 19], atomic and frequency combs [20, 21], quantum entanglement [22] and so on.

In general, the group velocity of light pulses is dependent on the dispersion properties of a medium, and is given by the standard expression, $v_g = c/n_g$ and $n_g = n + \omega(\mathrm{d}n/\mathrm{d}\omega)$, where n is the refractive index of medium, c is the speed of light in vacuum and ω is the angular frequency of light field. Exactly, the effective refractive index of the medium for a light beam is therefore determined by $n = n_0 + n_2 I$, where n_0 is the linear refractive index and n_2 is the nonlinear coefficient of the medium, I is the light intensity. In the fact, early studies on light group velocity in traditional medium often overlooked the nonlinear component (n_2), however, for the EIT medium with giant nonlinearity we need to consider the effect of nonlinear dispersion on the group velocity of light. Indeed, Xiao *et al* [23] considered the effect of self-Kerr nonlinearity on the group index and shown that due to the greatly enhanced nonlinear dispersion near resonance and an opposite sign (anomalous dispersion) from the linear dispersion therefore it obstructs the slowing down of light. Meanwhile, Dey and Agarwal [24] studied the effect of cross-Kerr nonlinearity on the slow light propagation through a four-level N-type system under an EIT condition. Their numerical results clearly show the group index of the probe field changes significantly due to the presence of Kerr nonlinearity.

Early research works on the effect of Kerr nonlinearity on group velocity have been investigated in three- or four- level atomic systems with single transparent window [23, 24], therefore, the group velocity is only manipulated in a narrow spectrum region corresponding to the EIT window. However, recent studies have focused on multi-level atomic systems to

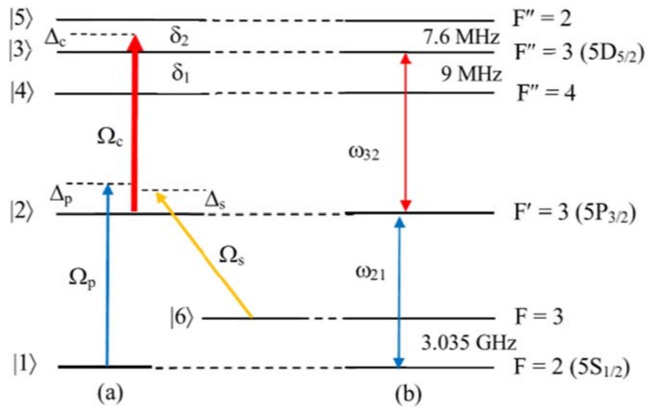

Figure 1. (a) Schematic diagram of the six-level inverted-Y system, (b) energy level diagram of ^{85}Rb atom.

create multiple EIT windows [25–29], and therefore the group velocity [30–32] as well as giant Kerr-nonlinearity [33–37] is also controlled at multiple frequency regions. Very recently, we have investigated the effect of self-Kerr nonlinearity on light group velocity in a five-level cascade system [38]. It is shown that the effect of self-Kerr nonlinearity can reduce the group index or enhance the group velocity of the probe light.

Along with this interest, in this paper, we propose an analytical method to study the effect of cross-Kerr nonlinearity on group velocity of probe light in a six-level inverted-Y atomic medium. This configuration has several interesting features: firstly, it is possible to generate three EIT windows therefore the giant Kerr nonlinearity and the group index can be controlled at multiple frequencies; secondly, the configuration uses closely-spaced hyperfine levels excited by just one coupling laser field instead of using three coupling laser fields (for creating three-EIT windows), so that it can be advantageous for experimental observation and investigating related applications. By deriving the expression of group index associated with cross-Kerr nonlinear coefficient for probe light, we consider the dependence of group index for the probe light on the coupling and signal lights and then show possible ways to switch the propagation of probe light between the subluminal and superluminal modes in different frequency regions. Such analytical model is not only convenient for investigating the influence of laser parameters on group velocity but is also easy used to fit the experimental results.

2. Theoretical model

The six-level inverted-Y atomic system interacting with three laser beams is shown in figure 1(a), which can be experimentally realized in Rb atoms (b). A weak probe laser beam, Ω_p drives the transition $|1\rangle \leftrightarrow |2\rangle$, whereas an intense coupling laser beam, Ω_c couples simultaneously transitions between the state $|2\rangle$ and three closely-spacing states $|3\rangle$, $|4\rangle$ and $|5\rangle$. The frequency separations between the levels $|3\rangle$–$|4\rangle$ and $|5\rangle$–$|3\rangle$ are δ_1 and δ_2, respectively. A signal laser beam, Ω_s is applied to the transition $|2\rangle \leftrightarrow |6\rangle$, here state $|6\rangle$ (and state $|1\rangle$) are hyperfine levels of ground state. The frequency detuning of the probe, coupling and signal lasers respectively defined as:

$$\Delta_c = \omega_c - \omega_{32},\ \ \Delta_p = \omega_p - \omega_{21} \text{ and } \Delta_s = \omega_s - \omega_{62} \quad (1)$$

with ω_p, ω_c and ω_s are the frequency of probe, coupling and signal beams, respectively.

The equation of the motion for the density operator describing an atomic system can be expressed as:

$$\frac{\partial \rho}{\partial t} = -\frac{\mathrm{i}}{\hbar}[H, \rho] + \Lambda\rho, \quad (2)$$

where, H and $\Lambda\rho$ represent the total Hamiltonian and the relaxation term, respectively. The total Hamiltonian of the system in the interaction picture can be written as [38]:

$$H = \frac{\hbar}{2}\begin{pmatrix} 0 & \Omega_p & 0 & 0 & 0 & 0 \\ \Omega_p & 2(\Delta_p - \Delta_s) & \Omega_c a_{32} & \Omega_c a_{42} & \Omega_c a_{52} & \Omega_s \\ 0 & \Omega_c a_{32} & 2(\Delta_p + \Delta_c) & 0 & 0 & 0 \\ 0 & \Omega_c a_{42} & 0 & 2(\Delta_p + \Delta_c + \delta_1) & 0 & 0 \\ 0 & \Omega_c a_{52} & 0 & 0 & 2(\Delta_p + \Delta_c - \delta_2) & 0 \\ 0 & \Omega_s & 0 & 0 & 0 & 0 \end{pmatrix}, \quad (3)$$

From equations (2) and (3) we derive the following equations of motion for the density matrix elements:

$$\dot{\rho}_{66} = -\Gamma_{62}\rho_{66} + \frac{\mathrm{i}\Omega_s}{2}(\rho_{62} - \rho_{26}), \quad (4)$$

$$\dot{\rho}_{55} = -\Gamma_{52}\rho_{55} + \frac{\mathrm{i}}{2}\Omega_c a_{52}(\rho_{52} - \rho_{25}), \quad (5)$$

$$\dot{\rho}_{44} = -\Gamma_{42}\rho_{44} + \frac{\mathrm{i}}{2}\Omega_c a_{42}(\rho_{42} - \rho_{24}), \quad (6)$$

$$\dot{\rho}_{33} = -\Gamma_{32}\rho_{33} + \frac{\mathrm{i}}{2}\Omega_c a_{32}(\rho_{32} - \rho_{23}), \quad (7)$$

$$\begin{aligned}\dot{\rho}_{22} = &-\Gamma_{21}\rho_{22} + \Gamma_{32}\rho_{33} + \Gamma_{42}\rho_{44} + \Gamma_{52}\rho_{55} \\ &+ \Gamma_{62}\rho_{66} + \frac{\mathrm{i}}{2}\Omega_p(\rho_{21} - \rho_{12}) + \frac{\mathrm{i}}{2}\Omega_c a_{32}(\rho_{23} - \rho_{32}) \\ &+ \frac{\mathrm{i}}{2}\Omega_c a_{42}(\rho_{24} - \rho_{42}) + \frac{\mathrm{i}}{2}\Omega_c a_{52}(\rho_{25} - \rho_{52}) \\ &+ \frac{\mathrm{i}}{2}\Omega_s(\rho_{26} - \rho_{62}),\end{aligned} \quad (8)$$

$$\dot{\rho}_{11} = \Gamma_{21}\rho_{22} + \frac{\mathrm{i}}{2}\Omega_p(\rho_{12} - \rho_{21}), \tag{9}$$

$$\dot{\rho}_{21} = [\mathrm{i}\Delta_p - \gamma_{21}]\rho_{21} + \frac{\mathrm{i}}{2}\Omega_p(\rho_{22} - \rho_{11}) - \frac{\mathrm{i}}{2}\Omega_c a_{32}\rho_{31} - \frac{\mathrm{i}}{2}\Omega_c a_{42}\rho_{41} - \frac{\mathrm{i}}{2}\Omega_c a_{52}\rho_{51} - \frac{\mathrm{i}}{2}\Omega_s\rho_{61}, \tag{10}$$

$$\dot{\rho}_{31} = [\mathrm{i}(\Delta_c + \Delta_p) - \gamma_{31}]\rho_{31} + \frac{\mathrm{i}}{2}\Omega_p\rho_{32} - \frac{\mathrm{i}}{2}\Omega_c a_{32}\rho_{21}, \tag{11}$$

$$\dot{\rho}_{41} = [\mathrm{i}(\Delta_c + \Delta_p + \delta_1) - \gamma_{41}]\rho_{41} + \frac{\mathrm{i}}{2}\Omega_p\rho_{42} - \frac{\mathrm{i}}{2}\Omega_c a_{42}\rho_{21}, \tag{12}$$

$$\dot{\rho}_{51} = [\mathrm{i}(\Delta_c + \Delta_p - \delta_2) - \gamma_{51}]\rho_{51} + \frac{\mathrm{i}}{2}\Omega_p\rho_{52} - \frac{\mathrm{i}}{2}\Omega_c a_{52}\rho_{21}, \tag{13}$$

$$\dot{\rho}_{61} = [\mathrm{i}(\Delta_s - \Delta_p) - \gamma_{61}]\rho_{61} + \frac{\mathrm{i}}{2}\Omega_p\rho_{62} - \frac{\mathrm{i}}{2}\Omega_s\rho_{21}, \tag{14}$$

$$\dot{\rho}_{32} = [\mathrm{i}\Delta_c - \gamma_{32}]\rho_{32} + \frac{\mathrm{i}}{2}\Omega_p\rho_{31} + \frac{\mathrm{i}}{2}\Omega_c a_{42}\rho_{34} + \frac{\mathrm{i}}{2}\Omega_c a_{52}\rho_{35} + \frac{\mathrm{i}}{2}\Omega_c a_{32}(\rho_{33} - \rho_{22}) + \frac{\mathrm{i}}{2}\Omega_s\rho_{36}, \tag{15}$$

$$\dot{\rho}_{42} = [\mathrm{i}(\Delta_c + \delta_1) - \gamma_{42}]\rho_{42} + \frac{\mathrm{i}}{2}\Omega_p\rho_{41} + \frac{\mathrm{i}}{2}\Omega_c a_{32}\rho_{43} + \frac{\mathrm{i}}{2}\Omega_c a_{52}\rho_{45} + \frac{\mathrm{i}}{2}\Omega_c a_{42}(\rho_{44} - \rho_{22}) + \frac{\mathrm{i}}{2}\Omega_s\rho_{46}, \tag{16}$$

$$\dot{\rho}_{52} = [\mathrm{i}(\Delta_c - \delta_2) - \gamma_{52}]\rho_{52} + \frac{\mathrm{i}}{2}\Omega_p\rho_{51} + \frac{\mathrm{i}}{2}\Omega_c a_{32}\rho_{53} + \frac{\mathrm{i}}{2}\Omega_c a_{42}\rho_{54} + \frac{\mathrm{i}}{2}\Omega_c a_{52}(\rho_{55} - \rho_{22}) + \frac{\mathrm{i}}{2}\Omega_s\rho_{56}, \tag{17}$$

$$\dot{\rho}_{62} = [\mathrm{i}\Delta_s - \gamma_{26}]\rho_{62} - \frac{\mathrm{i}}{2}\Omega_s(\rho_{22} - \rho_{66}) + \frac{\mathrm{i}}{2}\Omega_P\rho_{61} + \frac{\mathrm{i}\Omega_c}{2}a_{32}\rho_{63} + \frac{\mathrm{i}\Omega_c}{2}a_{42}\rho_{64} + \frac{\mathrm{i}\Omega_c}{2}a_{52}\rho_{65}, \tag{18}$$

$$\dot{\rho}_{43} = [-\mathrm{i}\delta_1 - \gamma_{43}]\rho_{43} + \frac{\mathrm{i}}{2}\Omega_c a_{32}\rho_{42} - \frac{\mathrm{i}}{2}\Omega_c a_{42}\rho_{23}, \tag{19}$$

$$\dot{\rho}_{53} = [-\mathrm{i}\delta_2 - \gamma_{53}]\rho_{53} + \frac{\mathrm{i}}{2}\Omega_c a_{32}\rho_{52} - \frac{\mathrm{i}}{2}\Omega_c a_{52}\rho_{23}, \tag{20}$$

$$\dot{\rho}_{63} = [\mathrm{i}(\Delta_s - \Delta_c) - \gamma_{36}]\rho_{63} + \frac{\mathrm{i}}{2}\Omega_c a_{32}\rho_{62} - \frac{\mathrm{i}}{2}\Omega_s\rho_{23}, \tag{21}$$

$$\dot{\rho}_{54} = [-\mathrm{i}(\delta_1 + \delta_2) - \gamma_{54}]\rho_{54} + \frac{\mathrm{i}}{2}\Omega_c a_{42}\rho_{52} - \frac{\mathrm{i}}{2}\Omega_c a_{52}\rho_{24}, \tag{22}$$

$$\dot{\rho}_{64} = [\mathrm{i}(\Delta_c - \Delta_s + \delta_1) - \gamma_{46}]\rho_{64} + \frac{\mathrm{i}}{2}\Omega_c a_{42}\rho_{62} - \frac{\mathrm{i}}{2}\Omega_s\rho_{24}, \tag{23}$$

$$\dot{\rho}_{65} = [-\mathrm{i}(\Delta_c - \Delta_s - \delta_1) - \gamma_{56}]\rho_{65} + \frac{\mathrm{i}}{2}\Omega_c a_{52}\rho_{62} - \frac{\mathrm{i}}{2}\Omega_s\rho_{25}, \tag{24}$$

The above equations are to be supplemented by $\rho_{ki} = \rho_{ik}^*$ and $\rho_{11} + \rho_{22} + \rho_{33} + \rho_{44} + \rho_{55} + \rho_{66} = 1$.

where, $\Omega_p = d_{21}E_p/\hbar$, $\Omega_c = d_{32}E_c/\hbar$ and $\Omega_s = d_{26}E_s/\hbar$; d_{kl} is element of dipole moment of the $|k\rangle$–$|l\rangle$ transition; $a_{32} = d_{32}/d_{32}$, $a_{42} = d_{42}/d_{32}$ and $a_{52} = d_{52}/d_{32}$ are the relative transition strengths; Γ_{kl} is the decay rate of population from level $|k\rangle$ to level $|l\rangle$, and γ_{kl} is the decay rate of the atomic coherence ρ_{kl}.

In a weak field limit of the probe light intensity, the solution for the matrix element ρ_{21} to the first order in the probe field Ω_p and to all order in coupling field Ω_c and signal field Ω_s is found as:

$$\rho_{21} = \frac{\mathrm{i}\Omega_p/2}{(\mathrm{i}\Delta_p - \gamma_{21}) + \Omega_c^2(A + B + C) + \Omega_s^2 D}, \tag{25}$$

where A, B, C and D are controllable parameters given by

$$A = \frac{a_{32}^2}{4[\mathrm{i}(\Delta_p + \Delta_c) - \gamma_{31}]}, \tag{26}$$

$$B = \frac{a_{42}^2}{4[\mathrm{i}(\Delta_P + \Delta_c + \delta_1) - \gamma_{41}]}, \tag{27}$$

$$C = \frac{a_{52}^2}{4[\mathrm{i}(\Delta_P + \Delta_c - \delta_2) - \gamma_{51}]}, \tag{28}$$

$$D = \frac{1}{4[\mathrm{i}(\Delta_p + \Delta_s) - \gamma_{61}]}, \tag{29}$$

The susceptibility of the atomic medium for the probe field is given by

$$\chi = -\frac{N{d_{21}}^2}{\hbar\varepsilon_0}\frac{\mathrm{i}}{\mathrm{i}\Delta_p - \gamma_{21} + \Omega_c^2(A + B + C) + \Omega_s^2 D}, \tag{30}$$

where, N is density of particles, ε_0 is the permittivity in vacuum and E_p is electric field of probe light.

In the other hand, the total susceptibility in equation (30) can be written in an alternative form as [39]:

$$\chi = \chi^{(1)} + 3E_s^2\chi^{(3)}, \tag{31}$$

with E_s is electric field of signal light.

In order to extract the linear and nonlinearity terms, we make Taylor expansion in Ω_s of the susceptibility (30) to give the linear and nonlinearity terms:

$$\chi^{(1)} = -\frac{\mathrm{i}Nd_{21}^2}{\varepsilon_0\hbar}\frac{1}{(\mathrm{i}\Delta_p - \gamma_{21}) + {\Omega_c}^2(A + B + C)}, \tag{32}$$

$$\chi^{(3)} = \frac{\mathrm{i}Nd_{21}^2 d_{62}^2}{3\hbar^3\varepsilon_0}\frac{D}{[(\mathrm{i}\Delta_p - \gamma_{21}) + {\Omega_c}^2(A + B + C)]^2}, \tag{33}$$

From the linear and third order susceptibility, we found the linear index n_0 and cross-Kerr nonlinearity n_2 for the probe light as [39]:

$$n_0 = 1 + \frac{\mathrm{Re}\,(\chi^{(1)})}{2}, \tag{34}$$

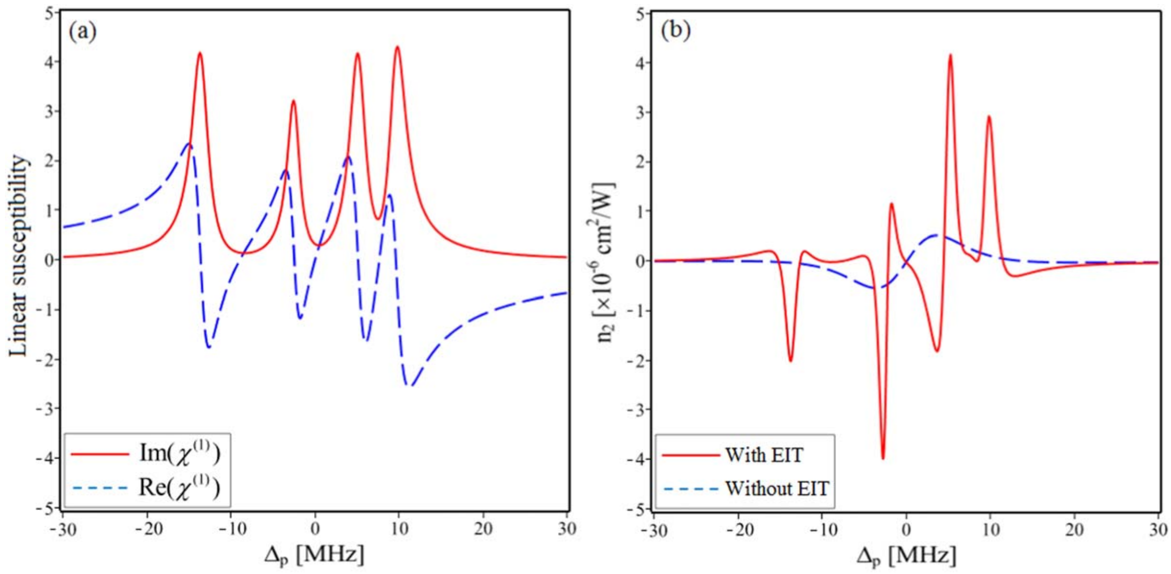

Figure 2. (a) Change of linear absorption (solid line) and linear dispersion (dashed line) versus probe frequency detuning Δ_p. (b) Change of Kerr coefficient n_2 versus frequency detuning of probe light when $\Omega_c = 10$ MHz (solid line) and $\Omega_c = 0$ (dashed line) with $\Delta_c = \Delta_s = 0$.

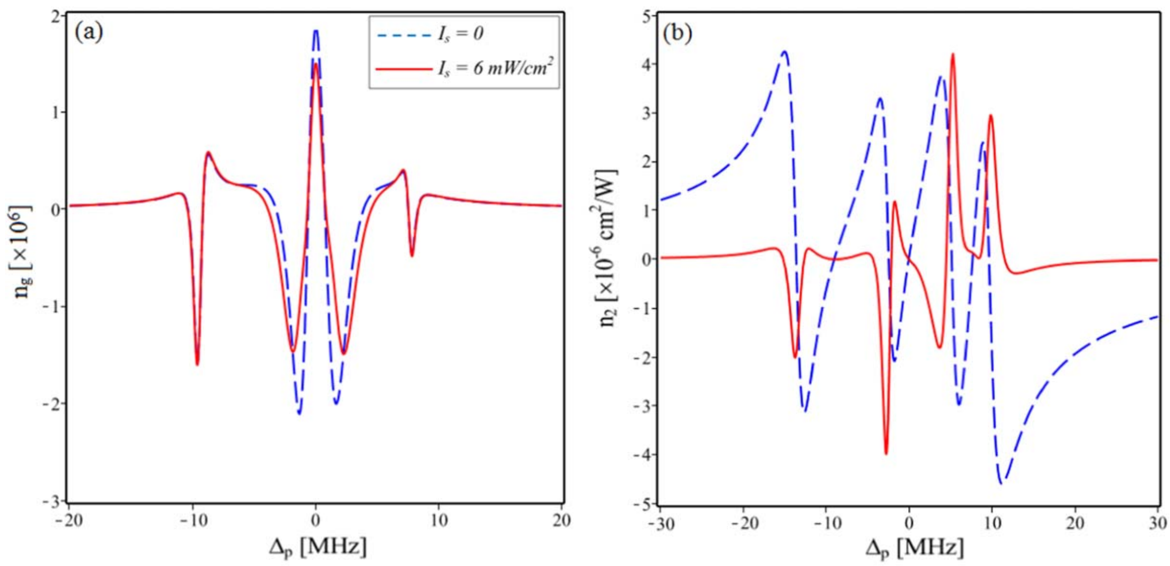

Figure 3. (a) Change of the group index versus probe frequency detuning Δ_p in the case of cross-Kerr nonlinearity absents (dashed line) and presents (solid line) when $I_s = 6$ mW cm^{-2}, $\Omega_c = 4$ MHz and $\Delta_c = \Delta_s = 0$. (b) Changes of the cross-Kerr nonlinearity n_2 (solid line) and linear index of refraction n_0 (dashed line) versus the probe frequency detuning Δ_p when $\Omega_c = 10$ MHz and $\Delta_c = \Delta_s = 0$.

$$n_2 = \frac{3\,\mathrm{Re}\,(\chi^{(3)})}{2\varepsilon_0 n_0^2 c}. \tag{35}$$

In the presence of cross-Kerr nonlinearity, the effective index of the atomic medium for the probe light is determined by [39]:

$$n = n_0 + n_2 I_s. \tag{36}$$

with I_s is the signal laser intensity.

The group index of the atomic medium for the probe light can therefore be calculated as:

$$n_g = n + \omega_p \frac{\partial n}{\partial \omega_p} \equiv n_0 + n_2 I_s + \omega_p \left(\frac{\partial n_0}{\partial \omega_p} + \frac{\partial n_2}{\partial \omega_p} I_s \right), \tag{37}$$

here, n_0 and n_2 are calculated from the expressions (34) and (35), respectively. We note here that the group index n_g in equation (37) is proportional to the signal intensity I_s, while n_g in [40] is proportional to the probe intensity I_p.

The group velocity v_g of the probe field is determined by:

$$v_g = \frac{c}{n_g}. \tag{38}$$

3. Results and discussion

In this section, we apply the calculation results to cold ^{85}Rb atoms in which Doppler broadening can be ignored. The level diagram of ^{85}Rb atom indicated as in figure 1(b) with the states, $|1\rangle$, $|6\rangle$, $|2\rangle$, $|3\rangle$, $|4\rangle$ and $|5\rangle$ are chosen as $5S_{1/2}(F = 2)$, $5S_{1/2}(F = 3)$, $5P_{3/2}(F' = 3)$, $5D_{5/2}(F'' = 3)$, $5D_{5/2}(F'' = 4)$, and $5D_{5/2}(F'' = 3)$, respectively. The atomic parameters are [25, 41]: $N = 10^{12}$ atoms cm^{-3}, $\Gamma_{32} = \Gamma_{42} = \Gamma_{52} = 0.97$ MHz, $\Gamma_{21} = \Gamma_{62} = 6$ MHz, $\delta_1 = 9$ MHz, $\delta_2 = 7.6$ MHz, $d_{21} = 1.6 \times 10^{-29}$ C m, $\omega_p = 3.77 \times 10^8$ MHz and a_{32}: a_{42}: $a_{52} = 1$:1.4:0.6.

First of all, we investigate the variation of linear absorption and dispersion versus probe frequency detuning in the presence of coupling field with $\Omega_c = 10$ MHz and $\Delta_c = 0$ as shown in figure 2(a). From the solid curve in figure 2(a), we can see that there are three EIT windows appear at the positions $\Delta_p = 0$, $\Delta_p = -9$MHz and $\Delta_p = 7.6$ MHz. Correspondingly, normal dispersion curves are also present in the three EIT windows as indicated by the dashed line in figure 2(a), therefore the group velocity can be controlled at these frequency regions. In figure 2(b) we consider the variation of Kerr nonlinearity n_2 with the respect to probe frequency detuning in two cases of the presence (solid line) and absence (dashed line) of EIT effect. From figure shows that cross-Kerr nonlinearity is significantly enhanced around three transparent spectral regions at the positions $\Delta_p = 0$, $\Delta_p = -9$ MHz and $\Delta_p = 7.6$ MHz. Namely, in each transparent window there is a pair of positive-negative peaks of n_2.

In order to see the effect of cross-Kerr nonlinearity on group velocity, we plot the group index versus the probe frequency detuning in the absence (dashed line) and presence (solid line) of cross-Kerr nonlinearity as displayed in figure 3(a). Here, the coupling frequency is resonant with the transition $|2\rangle \leftrightarrow |3\rangle$, i.e. $\Delta_c = 0$, and $\Omega_c = 3$ MHz while the intensity of signal laser is chosen as $I_s = 6$ mW cm^{-2} ($\Omega_s = 0.78$ MHz). It shows that there are three frequency regions centered at $\Delta_p = -9$ MHz, $\Delta_p = 0$, and $\Delta_p = 7.6$ MHz have normal dispersion therefore the group index is large and positive in each region. This means that the probe light can be slowed down simultaneously at three transparent frequency regions. However, the effect of cross-Kerr nonlinearity reduces the effective index and hence enhances the group velocity of the probe light (see the solid line in figure 3(a)) which is similar to the effect of self-Kerr nonlinearity (see [40]). In order to explain this phenomenon, we also plot the cross-Kerr nonlinearity n_2 (solid line) and linear index of refraction n_0 (dashed line) versus the probe frequency detuning Δ_p as in figure 3(b). It is clear that the linear dispersion $(\partial n_0/\partial \omega_p)$ is opposite sign with the nonlinear dispersion $(\partial n_2/\partial \omega_p)$ which leads to a decrease in the effective refractive index of the medium for the probe light.

In figure 4 we consider the influence of intensity of coupling and signal fields on the group index by plotting the group index versus the Rabi frequency of coupling field Ω_c at different values of the signal laser intensity for three EIT windows centered at $\Delta_p = 0$ (a), $\Delta_p = 7.6$ MHz (b) and $\Delta_p = -9$ MHz (c). It is shows that, when the signal laser intensity is small ($I_s = 6$ mW cm^{-2}), the effect of cross-Kerr nonlinearity on the group index for the probe laser at EIT windows $\Delta_p = 7.6$ MHz and $\Delta_p = -9$ MHz is also small,

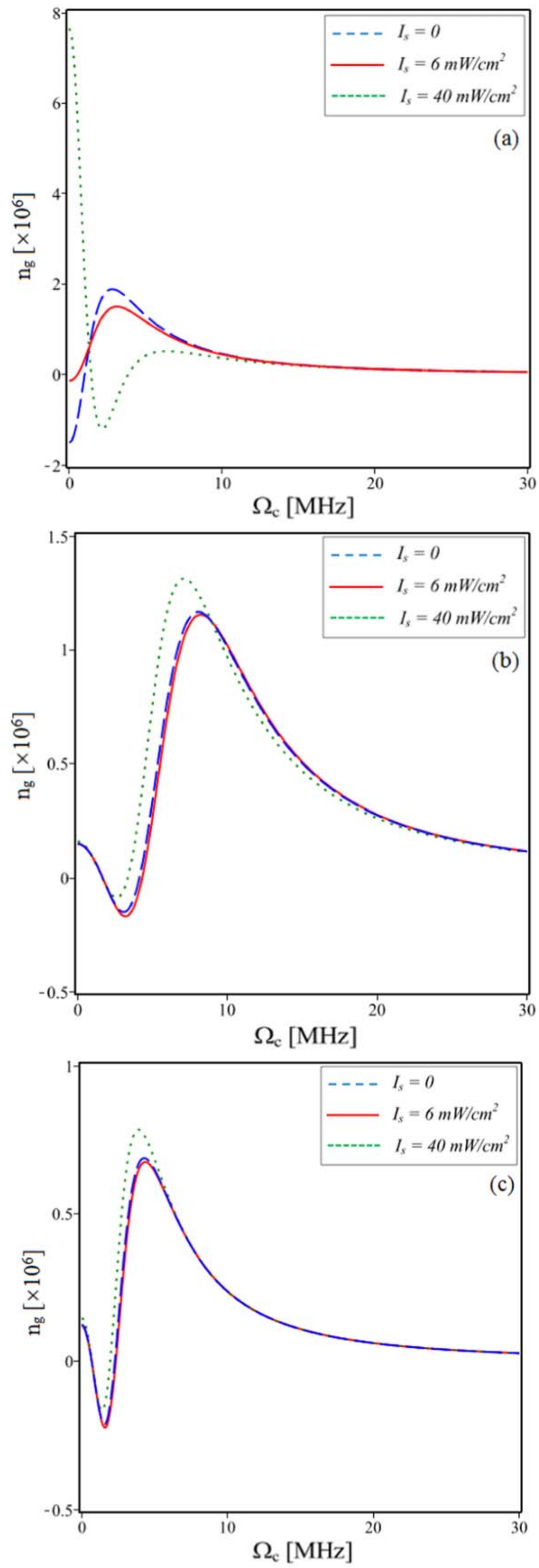

Figure 4. Changes of the group index versus Ω_c at different values of the signal laser intensity $I_p = 0$ (dashed line), $I_s = 6$ mW cm^{-2} (solid line), $I_s = 40$ mW cm^{-2} (dotted line) for three EIT windows centered at $\Delta_p = 0$ (a), $\Delta_p = 7.6$ MHz (b) and $\Delta_p = -9$ MHz (c). Other parameters are $\Delta_c = \Delta_s = 0$.

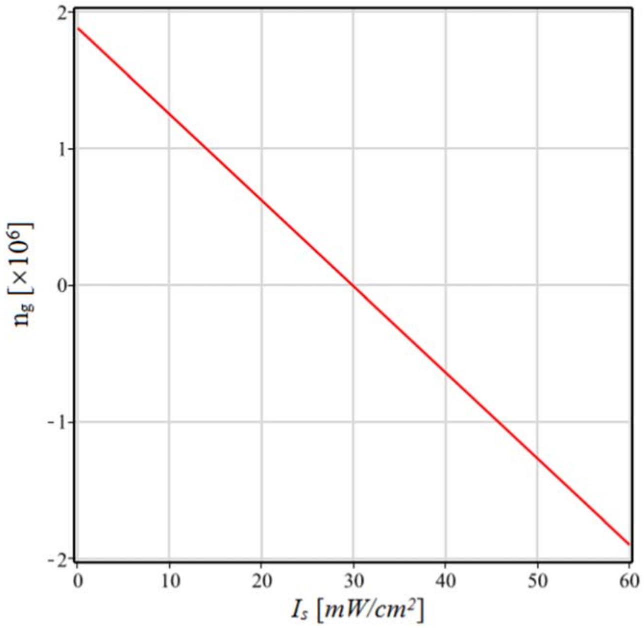

Figure 5. Change of the group index versus signal intensity I_s when $\Omega_c = 3$ MHz and $\Delta_c = \Delta_p = \Delta_s = 0$.

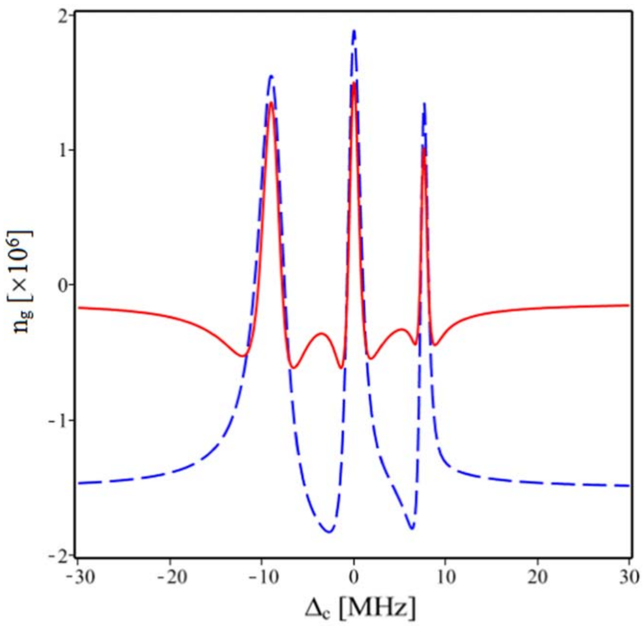

Figure 6. (a) Change of the group index versus coupling frequency detuning Δ_c in the case of cross-Kerr nonlinearity absents (dashed line) and presents (solid line) when $I_s = 6\,\text{mW cm}^{-2}$, $\Omega_c = 3$ MHz and $\Delta_c = \Delta_s = 0$.

but for EIT window at $\Delta_p = 0$ there is a significant deviation between the two curves (see the solid and dashed lines). When the signal laser intensity is increased to $40\,\text{mW cm}^{-2}$ ($\Omega_s = 3$ MHz), the effect of cross-Kerr nonlinearity on group index becomes apparent at the three EIT windows, particularly at the EIT window $\Delta_p = 0$, the sign of the group index switched from positive to negative and vice versa. In all cases, the influence of cross-Kerr nonlinearity can be negligible as the coupling laser intensity is much stronger than the signal laser intensity.

Thus, the influence of cross-Kerr nonlinearity leads to variation of both magnitude and sign of the group index under changing the signal field intensity, therefore one may manipulate the probe light propagation between sub- and supper-luminal modes by tuning the intensity of signal field, as in figure 5. For the selected parameters as shown in figure 5, the value of the group index can change from positive to negative when the signal laser intensity is greater than $30\,\text{mW cm}^{-2}$.

Finally, we consider the variations of group index versus the coupling frequency detuning in the absence (dashed line) and presence (solid line) of cross-Kerr nonlinearity as illustrated in figure 6. Here, the parameters are chosen as $\Omega_c = 3$ MHz, $I_s = 6\,\text{mW cm}^{-2}$ and $\Delta_p = \Delta_s = 0$. From figure we see that by changing the frequency of the coupling field, the group index also varies between negative and positive values. Moreover, there is a significant deviation between the two curves in the cases of the absence and presence of cross-Kerr nonlinearity, namely, the value of group index is considerably reduced when cross-Kerr nonlinearity is present.

4. Conclusion

We have studied the effect of giant Kerr nonlinearity on group velocity for probe light in a six-level inverted-Y atomic medium. Under EIT condition, the cross-Kerr nonlinearity is basically modified and enhanced greatly around in three spectral regions corresponding to transparent windows. Such a giant Kerr nonlinearity changes significantly group index of the medium for the probe light that leads to enhancement of group velocity. However, in the presence of cross-Kerr nonlinearity we can use the signal and/or coupling fields as knobs to control the group velocity of probe light between subluminal and superluminal in three transparent frequency regions. The analytical result not only gives sufficient knowledge on the effect of cross-Kerr nonlinearity on the group velocity, but is also convenient to make direct comparisons with experiments and supports future studies.

ORCID iDs

Le Van Doai https://orcid.org/0000-0002-1850-3437

References

[1] Harris S E 1997 *Phys. Today* **50** 36
[2] Schmidt H and Imamogdlu A 1996 *Opt. Lett.* **21** 1936
[3] Li S J, Yang X D, Cao X M, Zhang C H, Xie C D and Wang H 2008 *Phys. Rev. Lett.* **101** 073602
[4] Yang X D, Li S J, Zhang C H and Wang H 2009 *J. Opt. Soc. Am.* B **26** 1423–34
[5] Wang H, Goorskey D and Xiao M 2001 *Phys. Rev. Lett.* **87** 073601
[6] Doai L V, Khoa D X and Bang N H 2015 *Phys. Scr.* **90** 045502

[7] Agarwal G S, Dey T N and Menon S 2001 *Phys. Rev.* A **64** 053809
[8] Sun H, Guo H, Bai Y, Han D, Fan S and Chen X 2005 *Phys. Lett.* A **335** 68–75
[9] Mahmoudi M, Sahrai M and Tajalli H 2006 *Phys. Lett.* A **357** 66–71
[10] Bae I H and Moon H S 2011 *Phys. Rev.* A **83** 053806
[11] Bharti V and Natarajan V 2017 *Opt. Commun.* **392** 180–4
[12] Ottaviani C, Vitali D, Artoni M, Cataliotti F and Tombesi P 2003 *Phys. Rev. Lett.* **90** 197902
[13] Rebic Cataliotti S and Corbalán R 2004 *Phys. Rev.* A **70** 032317
[14] Joshi A and Xiao M 2005 *Phys. Rev.* A **72** 062319
[15] Lin Q and Li J 2009 *Phys. Rev.* A **79** 022301
[16] Hamedi H R and Juzeliunas G 2015 *Phys. Rev.* A **91** 053823
[17] Xu D, Bai Z and Huang G 2016 *Phys. Rev.* A **94** 063857
[18] Tan C and Huang G 2015 *Phys. Rev.* A **91** 023803
[19] Asgarnezhad-Zorgabad S, Sadighi-Bonabi R and Sanders B C 2018 *Phys. Rev.* A **98** 013825
[20] Teja G P, Simon C and Goyal S K 2019 *Phys. Rev.* A **99** 052314
[21] Asgarnezhad-Zorgabad S, Berini P and Sanders B C 2019 *Phys. Rev.* A **99** 051802(R)
[22] Zhu C and Huang G 2011 *Opt. Exp.* **19** 23364
[23] Wu H and Xiao M 2007 *Opt. Lett.* **32** 3122–4
[24] Dey T N and Agarwal G S 2007 *Phys. Rev.* A **76** 015802
[25] Doai L V, Trong P V, Khoa D X and Bang N H 2014 *Optik* **125** 3666–9
[26] Kumar R, Gokhroo V and Chormaic S N 2015 *New J. Phys.* **17** 123012
[27] Khoa D X, Trong P V, Doai L V and Bang N H 2016 *Phys. Scr.* **91** 035401
[28] Xu W and DeMarco B 2016 *Phys. Rev.* A **93** 011801
[29] Khoa D X, Trung L C, Thuan P V, Doai L V and Bang N H 2017 *J. Opt. Soc. Am.* B **34** 1255–63
[30] Han D, Zeng Y, Bai Y, Cao H, Chen W, Huang C and Lu H 2008 *Opt. Commun.* **281** 4712–4
[31] Yadav K and Wasan A 2017 *Phys. Lett.* A **381** 3246–53
[32] Tuan N A, Doai L V, Son D H and Bang N H 2018 *Optik* **171** 721–7
[33] Wang Z-B, Marzlin K-P and Sanders B C 2006 *Phys. Rev. Lett.* **97** 063901
[34] Khoa D X, Doai L V, Son D H and Bang N H 2014 *J. Opt. Soc. Am.* B **31** 1330
[35] Alotaibi H M M and Sanders B C 2015 *Phys. Rev.* A **91** 043817
[36] Alotaibi H M M and Sanders B C 2016 *Phys. Rev.* A **94** 053832
[37] Wang D, Liu C, Xiao C, Zhang J, Alotaibi H M M, Sanders B C, Wang L-G and Zhu S 2017 *Sci. Rep.* **7** 5796
[38] Doai L V, An N L T, Khoa D X, Sau V N and Bang N H 2019 *J. Opt. Soc. Am.* B **36** 2856–62
[39] Boyd R W 2008 *Nonlinear Optics* 3rd edn (New York: Academic)
[40] Anh N T, Doai L V and Bang N H 2018 *J. Opt. Soc. Am.* B **35** 1233–9
[41] Steck D A 2013 Rubidium 85 D Line Data (http://steck.us/alkalidata/)